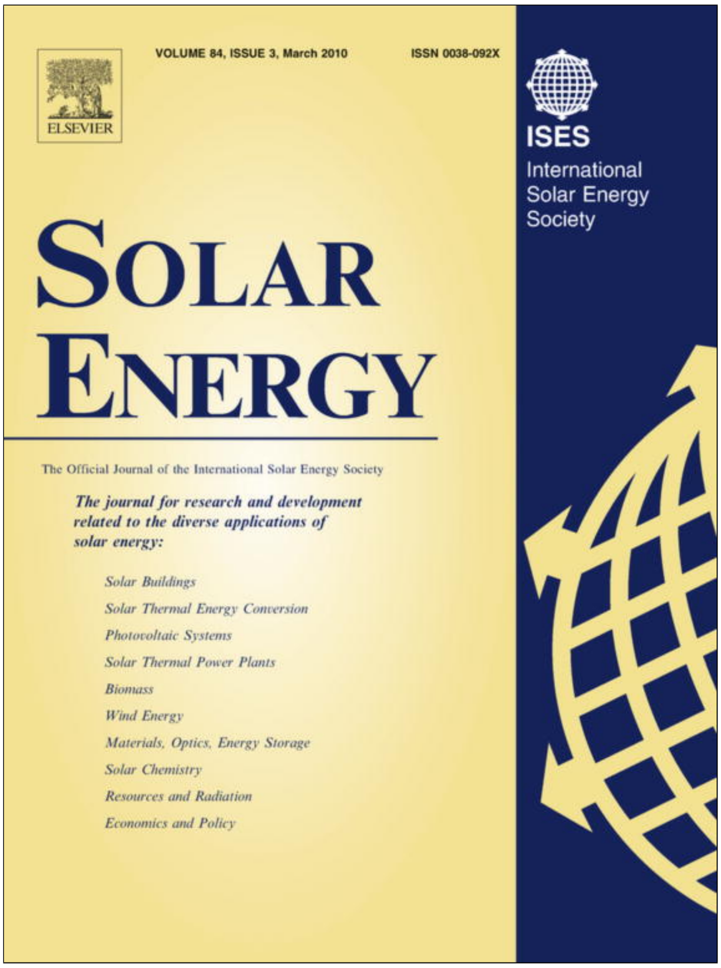

VOLUME 84, ISSUE 3, March 2010
ISSN 0038-092X
ELSEVIER

ISES
International
Solar Energy
Society

SOLAR ENERGY

The Official Journal of the International Solar Energy Society

The journal for research and development related to the diverse applications of solar energy:

- *Solar Buildings*
- *Solar Thermal Energy Conversion*
- *Photovoltaic Systems*
- *Solar Thermal Power Plants*
- *Biomass*
- *Wind Energy*
- *Materials, Optics, Energy Storage*
- *Solar Chemistry*
- *Resources and Radiation*
- *Economics and Policy*

Available online at www.sciencedirect.com
ScienceDirect
Solar Energy 84 (2010) 379–383
SOLAR ENERGY
www.elsevier.com/locate/solener

Temperature dependence of $Cu_2ZnSn(Se_xS_{1-x})_4$ monograin solar cells

J. Krustok *, R. Josepson, M. Danilson, D. Meissner

Tallinn University of Technology, Ehitajate tee 5, 19086 Tallinn, Estonia

Received 4 May 2009; received in revised form 17 September 2009; accepted 18 September 2009
Available online 16 December 2009

Communicated by: Associate Editor Takhir Razykov

Abstract

The temperature dependence of open-circuit voltage (V_{oc}), short-circuit current (I_{sc}), fill factor (FF), and relative efficiency of monograin $Cu_2ZnSn(Se_xS_{1-x})_4$ solar cell was measured. The light intensity was varied from 2.2 to 100 mW/cm^2 and temperatures were in the range of $T = 175–300$ K. With a light intensity of 100 mW/cm^2 dV_{oc}/dT was determined to be −1.91 mV/K and the dominating recombination process at temperatures close to room temperature was found to be related to the recombination in the space-charge region. The solar cell relative efficiency decreases with temperature by 0.013%/K. Our results show that the diode ideality factor n does not show remarkable temperature dependence and slightly increases from $n = 1.85$ to $n = 2.05$ in the temperature range between 175 and 300 K.

Keywords: $Cu_2ZnSn(Se_xS_{1-x})_4$; Solar cell; Temperature dependence; Monograin powder; I–V curves

1. Introduction

In recent years the quaternary CZTS-based semiconductors such as $Cu_2ZnSn(Se_xS_{1-x})_4$ have attracted increasing attention as possible absorber materials for solar cells. These materials have an optimal direct bandgap for solar energy conversion and a high absorption coefficient (>10^4 cm^{-1}) (Altosaar et al., 2008; Mellikov et al., 2008, 2009; Jimbo et al., 2007; Katagiri et al., 2009; Ennaoui et al., 2009). They are believed to be suitable alternatives for $CuInSe_2$ absorbers that contain expensive indium. These semiconductors can be obtained by replacing half of the indium atoms in chalcopyrite $CuInSe_2$ by zinc, and by replacing the other half by tin. While $CuInGaSe_2$- (CIGSe-) based solar cells show efficiencies of up to 20%, record efficiencies of thin film CZTSSe cells are as yet only about 6–7% (Katagiri et al., 2009). One possible reason for this is the fact that CZTSSe thin films often contain different binary and ternary phases. Therefore it seems to be more appropriate to use higher temperatures for growth in order to better control the phase composition of the product. This is one reason why so-called monograin solar cells (Altosaar et al., 2008; Mellikov et al.,2008, 2009) look very promising. At the same time many physical properties of these compounds are still unknown and also solar cells made on their basis have not been studied in detail. Especially important for further use of these materials is the temperature dependence of the solar cell parameters since solar cell performance generally decreases with increasing temperature, fundamentally due to increased internal carrier recombination rates, caused by increased carrier excitation. Large number of correlations expressing the temperature dependence of the PV module's electrical efficiency can be retrieved, although many of them assume the familiar linear form, differing only in the numerical values of the relevant parameters which are material and system dependent (Skoplaki and Palyvos, 2009; Amy and de la Breteque, 2009). Knowing these parameter is crucial for predicting the temperature dependence of CZTSSe modules also in the future. In this paper we will discuss detailed I/V-measurements of CZTSSe cells that were performed using various temperatures and light intensities.

---

* Corresponding author. Tel.: +372 620 3364.
E-mail address: krustok@staff.ttu.ee (J. Krustok).

0038-092X/$ - see front matter © 2009 Elsevier Ltd. All rights reserved.
doi:10.1016/j.solener.2009.09.011

2. Experimental

Monograin powder materials were synthesized from metal binaries (CuSe, ZnSe(S), SnSe and elemental Se) in a molten flux in an isothermal recrystallization process. The grounded precursors were thermally annealed in evacuated quartz ampoules. The crystal size of the materials was controlled by the temperature and duration of the recrystallization process and by the chemical nature of the flux. Surface morphology, phase structure and composition of the powder crystals were analyzed by high resolution SEM, XRD and EDS, respectively. The evolution of crystal shape and morphology of the monograin powders was analyzed by electron imaging using a high-resolution scanning electronmicroscope (SEM) Zeiss ULTRA55 with the compositional contrast detector EbS. The chemical composition and the distribution of components in powder crystals were determined using an energy dispersive X-ray analysis (EDX) system (Röntex). XRD patterns were recorded using a Bruker AXS D5005 diffractometer with the monochromatic Cu K_α-radiation.

Monograin layer (MGL) solar cells were made from grains with diameters of 56–63 µm as selected by sieving. The absorber material had a composition $Cu_{1.9}Zn_{1.01}$-$Sn(Se_{0.29}S_{0.71})_{3.88}$ as determined by energy dispersive X-ray analysis (EDS). This material was used for the formation of the absorber layer in the MGL solar cell structure: graphite/CZTSSe/CdS/ZnO (Altosaar et al., 2008; Mellikov et al., 2008, 2009). Powder crystals were covered with chemically deposited CdS buffer layers. For MGL formation a monolayer of CZTSSe powder crystals was glued together by a thin layer of epoxy. The polymer film thickness was adjusted to 20 µm on top of a 10 µm glue film before inserting the monograins. Since the grains sink into the polymer and reach the underneath glue layer, after washing off the glue completely, the lower part of each grain sticks out of the polymer film. After polymerization of this epoxy, i-ZnO and conductive ZnO:Al were deposited by RF-sputtering onto the open (i.e. not covered by epoxy) surface of the layer. Solar cell structures were completed by vacuum evaporation of 1–2 µm thick in grid contacts onto the ZnO window layer. Following this, the layer was glued onto glass substrates. The opening of back contact areas of crystals that were originally inside the epoxy was done by etching of the epoxy by H_2SO_4 and by additional abrasive treatment. This finalized the preparation of the solar cell structure. Graphite paste was used for the back contacts.

The prepared solar cells have an area of about 0.04 cm^2 and their solar efficiency was measured in a Oriel class A solar simulator (19159A, Newport) to be in the range of 5%.

I–V curves were measured using an Autolab PGSTAT system. The solar cells were mounted on the cold finger of a closed-cycle He cryostat (Janis) and the temperature of the cell was changed from 300 to 170 K with $\Delta T = 5$ K. As a light source we used a standard halogen lamp with calibrated intensity. The maximum intensity was 100 mW/cm^2. Lower intensities were realized by using spectrally neutral net filters.

3. Theory

The main temperature dependence in solar cells arises from variation of three main parameters, which are usually used to characterize the solar cell outputs (Green, 1982), these are: I_{sc}, the short-circuit current, which usually has a negative sign; the open-circuit voltage V_{oc} which in principal is characterized by I_o, the diode saturation current, and n, the diode ideality factor; and the fill factor FF, which in turn is a function of V_{oc}.

CZTSSe cells are not really ideal, and therefore it is necessary to take into account also series resistance R_S and parallel conductance G_{sh} of these cells. Then the solar cell equation will be given by

$$I = I_0\left[\exp\left(\frac{q(V - R_S I)}{nkT}\right) - 1\right] + G_{sh}(V - R_S I) - I_L \tag{1}$$

where I_L is the photocurrent, I_0 is the dark saturation current and n is the diode ideality factor, which can all be dependent on bias voltage and temperature. Usually, n has a value between 1 and 2, but values larger than 2 are also possible. In the case where there is no recombination in the space-charge region, n should have a value of 1. If on the other hand the current is dominated by recombination in the space-charge region, n should be 2.

V_{oc} we can obtain from Eq. (1) (taking $I = 0$):

$$V_{OC} = \frac{nkT}{q}\ln\left[1 - \frac{G_{sh}V_{oc}}{I_0} + \frac{I_L}{I_0}\right] \tag{2}$$

According to theory, I_0 is a function of material properties and it is also sensitive to temperature. In general (Green, 1982; Rau and Schock, 1999)

$$I_0 = I_{00}\exp\left[-\frac{E_A}{nkT}\right] \approx AT^3\exp\left[-\frac{E_A}{nkT}\right], \tag{3}$$

where the activation energy E_A and also I_{00} depend mainly on the dominating recombination mechanism in the solar cell. In case of bulk recombination $E_A \approx E_g$ where E_g is the bandgap energy of the absorber material.

According to (2) we expect a linear dependence of V_{oc} on temperature, if $I_L >> G_{sh}V_{oc}$ and $I_L >> I_0$. Then from (2) and (3) we have

$$V_{oc} = \frac{E_A}{q} - \frac{nkT}{q}\ln\left[\frac{I_{00}}{I_L}\right] \tag{4}$$

At the same time we must take into account that the ideality factor n and also I_{00} have a small but certain temperature dependence (Rau and Schock, 1999).

The photocurrent I_L of a solar cell generally increases slightly with increasing temperature, due to a decreasing bandgap energy. This decrease in the bandgap allows photons with longer wavelengths, lower energy, to be absorbed by the solar cell. As a result, the short-circuit current of the cell increases. In good solar cells $-I_L \approx I_{sc}$. In general, from Eq. (1) we find for I_{sc}

$$I_{sc} = I_0\left[\exp\left(-\frac{qR_S I_{sc}}{nkT}\right) - 1\right] - R_S I_{sc} G_{sh} - I_L \qquad (5)$$

It is practically impossible to calculate the T-dependence of I_{sc}, but in many cases we can assume a simple linear dependence. Again, if the series resistance of the cell becomes larger, then $|I_{sc}| < |I_L|$ and we will have a more complex dependence. The same is valid if the intensity (and therefore also $|I_{sc}|$) becomes larger and the exponential term in Eq. (5) starts to play a role.

In many cases it is possible to avoid complications from series resistance effects by using I_{sc} vs. V_{oc} curves measured for different light intensities and temperatures. Taking $I = 0$ Eq. (1) becomes

$$I_L = I_0\left[\exp\left(\frac{qV_{oc}}{nkT}\right) - 1\right] + G_{sh} V_{oc} \qquad (6)$$

If the shunting current is small and $I_L = -I_{sc}$ then we will have a simple exponential function. Using Eq. (6) we are able to extract I_0 and the ideality factor n.

Fill factors *FF* depend on a range of cell parameters, including current and voltage operating levels, cell ideality factors and parasitic series and shunt resistances. As such, it is difficult to derive generic formulae for the temperature sensitivity of this parameter. At the same time the temperature dependence of the fill factor often determines the shape of the temperature dependence curve of the power outcome of the solar cell, because both I_{sc} and V_{oc} usually show nearly linear behavior on temperature. In good solar cells and at higher temperatures *FF* usually decreases with temperature (Würfel, 2005). At lower temperatures, when R_{se} increases, *FF* usually shows an opposite dependence. Therefore we may expect a maximum value of *FF* somewhere below room temperatures.

4. Results and discussion

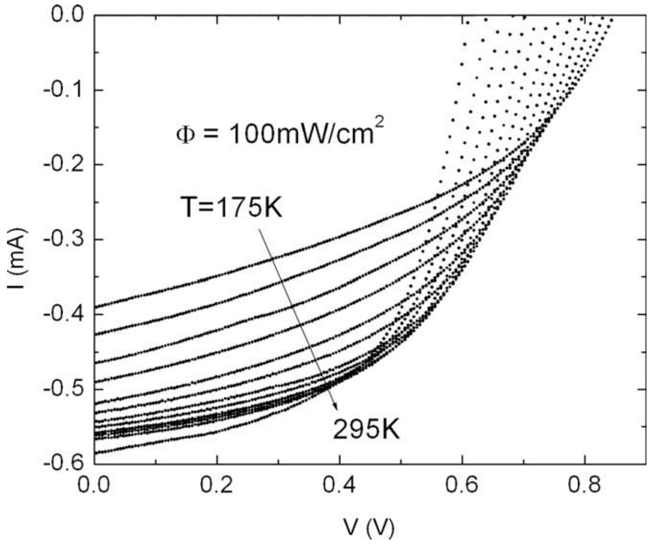

Fig. 1. Temperature dependence of I–V curves of CZTSSe monograin solar cells obtained in a light intensity of 100 mW/cm^2.

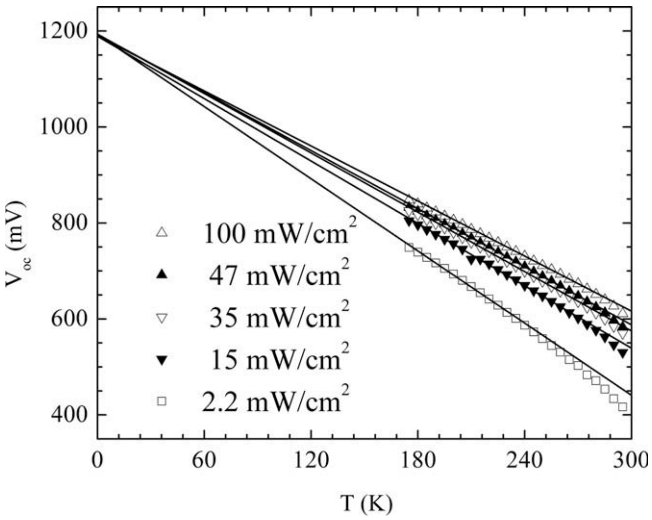

Fig. 2. Open circuit voltage V_{oc} of the CZTSSe monograin cell as a function of temperature illuminated with different light intensities. The straight lines are linear fits of Eq. (4).

In Fig. 1, I–V curves measured at different temperatures under 100 mW/cm^2 illumination are presented. It can be seen that increasing the temperature leads to a decrease of V_{oc} and an increase of I_{sc}.

The thermal behavior of the V_{oc} under different light intensities is shown in Fig. 2. As shown here, with an illumination intensity of 100 mW/cm^2 the open-circuit voltage V_{oc} increases with decreasing temperature by 1.91 mV/K. The linear behavior for all light intensities indicates that, according to Eq. (4), the temperature dependence of the ideality factor n and of I_{00} have only a minor effect on the temperature dependence of V_{oc}. According to theory, all V_{oc} (T) curves measured for different intensities must show different slopes but the same E_A at 0 K. The extrapolation to 0 K results in $E_A \approx 1.2$ eV for all intensities. This is consistent with the spectral response (Altosaar et al., 2008) and photoluminescence (Grossberg et al., 2009) measurements and shows that $E_A \approx E_g$ in this material. This in turn is direct evidence that in these CZTSSe monograin solar cells the dominating recombination (at least at temperatures close to room temperature) is a recombination in the space-charge region. All measured V_{oc} (T) curves were fitted with linear functions and the corresponding fitting parameters are given in Table 1.

Table 1
Parameters obtained from fitting temperature dependent I/V-curves.

Φ (mW/cm^2)	$-\frac{dV_{oc}}{dT}$ (mV/K)	E_A (meV)	$\frac{d\eta}{dT}$ (%/K)
100	1.91	1190	−0.013
47	2.02	1193	−0.016
35	2.06	1193	−0.020
15	2.17	1189	−0.022
2.2	2.51	1193	−0.025

We also observed linear increase of I_{sc} with temperature in the range 200–300 K. For 100 mW/cm^2 we found $dI_{sc}/dT = 6 \times 10^{-4}$ mA/K. At lower intensities this slope is even smaller.

According to Eq. (6), a semilogarithmic plot of I_{sc} versus V_{oc} will yield a straight line for high-enough V_{oc}. From this slope n can be calculated if one knows the temperature. I_0 can be found by taking the intercept of the straight part of the plot with the I_{sc}-axis. In Fig. 3 I_{sc} (V_{oc}) curves for different temperatures were plotted. It can be seen that all curves show a simple exponential behavior. All experimental curves were fitted using the exponential part of Eq. (6). Fitting results shows that the diode ideality factor n does not exhibits a remarkable temperature dependence and only slightly increases from $n = 1.85$ to $n = 2.05$ in the temperature range $T = 175$–300 K. This is a quite surprising result because in most solar cells the ideality factor decreases with temperature (Rau and Schock, 1999; Würfel, 2005). One reason for this different trend in our cells can be the temperature dependent bulk recombination current which increases at higher temperatures. Therefore we observe an ideality factor very close to $n = 2$.

From Fig. 3 we also extracted I_0 values and the temperature dependence of I_0 is shown in Fig. 4. We fitted these calculated points with Eq. (3), by using an average value on n ($n = 1.87$). Although this fitting is not very accurate we still got $E_A = 1.24$ eV and this value is very close to the E_A value we found using V_{oc} (T) curves. This coincidence supports assumptions we made regarding the role of G_{sh} and R_{se} and the use of a simplified theoretical model where we did not directly take into account the decrease of the bandgap energy with temperature.

Especially important is the temperature dependence of the relative efficiency η of solar cells. Therefore we plotted also η (T) curves measured at different light intensities, see Fig. 5. Calculated efficiencies are not calibrated, because we used a simple halogen light source and therefore AM1.5 spectral conditions were not followed. It can be seen that the efficiencies have a maximum value below room temperature. The corresponding maximum efficiency temperature increases with light intensity and at 100 mW/cm^2 it is at about 250 K. At low temperatures the efficiency starts to decrease with decreasing temperature. The same decrease can be observed also with increasing the temperature above 250 K. At this "high" temperature region the decrease of the efficiency is nearly linear with temperature. Corresponding slopes are also given in Table 1. This curved η (T) dependence is caused by the temperature dependence of the fill factor FF.

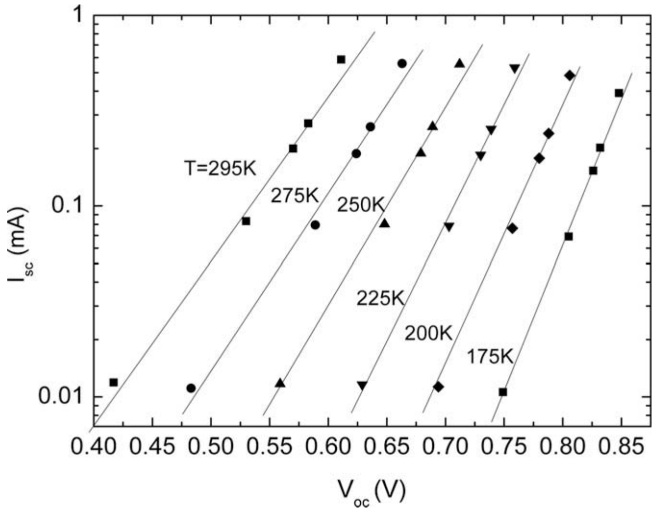

Fig. 3. I_{sc}/V_{oc}-curves for temperatures in the range of 175–295 K. Every measurement was done with five different illumination intensities ranging from 2.2 to 100 mW/cm^2. Lines represent the least square fit showing good correlation with Eq. (6).

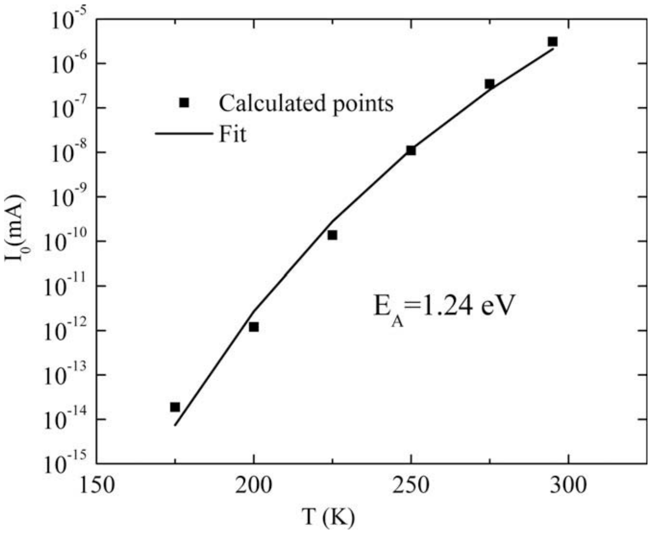

Fig. 4. I_0/T -graph. Experimental points were fitted using Eq. (3).

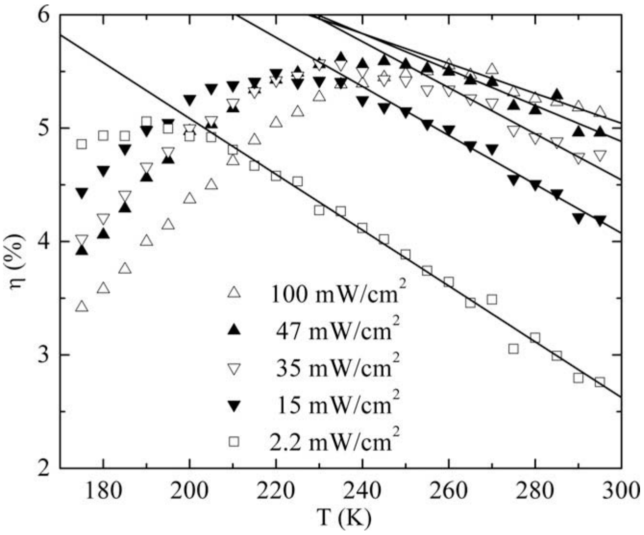

Fig. 5. Temperature dependence of the relative efficiency η of a CZTSSe monograin solar cell illuminated with different light intensities. Linear fitting was used for the high temperature region and fitting results are presented as lines.

Measured temperature coefficients of CZTSSe monograin solar cells indicate that in many cases they are lower than for other type of solar cells. For example Cu(In,Ga)Se$_2$ cells usually show dV_{oc}/dT values from −2.01 to −3.3 mV/K and $d\eta/dT$ values from −0.017 to −0.064%/K (Kniese et al., 2003). Si cells show dV_{oc}/dT values from −2.07 to −2.17 mV/K and $d\eta/dT$ value about −0.042%/K (Singh, 2008). The same is the situation in CdTe cells, where dV_{oc}/dT is typically in the range of −2.1 to −2.2 mV/K (Phillips et al., 1994). These low values of measured temperature coefficients of CZTSSe solar cells show a great potential of this compound.

5. Conclusions

In summary, from I–V measurements we have calculated the monograin $Cu_2ZnSn(Se_xS_{1-x})_4$ solar cell parameters as a function of temperature. For a light intensity of 100 mW/cm^2 the $dV_{oc}/dT = -1.91$ mV/K and E_A was close to the bandgap energy of 1.2 eV. The dominating recombination is related to recombination in the space-charge region. The solar cell relative efficiency decreases with temperature with a slope of 0.013%/K. The diode ideality factor n was close to a value of 2 and showed very small increase with temperature.

Acknowledgements

The authors thank the CZTSSe-team at the TUT. This work was supported by the Estonian Science Foundation Grant G-6554 and by the target financing by HTM (Estonia) No. SF0140099s08.

References

Altosaar, M., Raudoja, J., Timmo, K., Danilson, M., Grossberg, M., Krustok, J., Mellikov, E., 2008. $Cu_2\ Zn_{1-x}\ Cd_x\ Sn(Se_{1-y}\ S_y)_4$ solid solutions as absorber materials for solar cells. Physica Status Solidi A 205, 167–170.

Amy de la Breteque, E., 2009. Thermal aspects of c-Si photovoltaic module energy rating. Solar Energy 83, 1425–1433.

Ennaoui, A., Lux-Steiner, M., Weber, A., Abou-Ras, D., Kötschau, I., Schock, H.-W., Schurr, R., Hölzing, A., Jost, S., Hock, R., Voß, T., Schulze, J., Kirbs, A., 2009. Cu_2ZnSnS_4 thin film solar cells from electroplated precursors: novel low-cost perspective. Thin Solid Films 517, 2511–2514.

Green, M.A., 1982. Solar Cells. Prentice-Hall, Inc., Englewood Cliffs.

Grossberg, M., Krustok, J., Timmo, K., Altosaar, M., 2009. Radiative recombination in $Cu_2ZnSnSe_4$ monograins studied by photoluminescence spectroscopy. Thin Solid Films 517, 2489–2492.

Jimbo, K., Kimura, R., Kamimura, T., Yamada, S., Maw, W.S., Araki, H., Oishi, K., Katagiri, H., 2007. Cu_2ZnSnS_4-type thin film solar cells using abundant materials. Thin Solid Films 515, 5997–5999.

Katagiri, H., Jimbo, K., Maw, W.S., Oishi, K., Yamazaki, M., Araki, H., Takeuchi, A., 2009. Development of CZTS-based thin film solar cells. Thin Solid Films 517, 2455–2460.

Kniese, R., Hariskos, D., Voorwinden, G., Rau, U., Powalla, M., 2003. High band gap Cu(In, Ga)Se2 solar cells and modules prepared with in-line co-evaporation. Thin Solid Films 431–432, 543–547.

Mellikov, E., Altosaar, M., Krunks, M., Krustok, J., Varema, T., Volobujeva, O., Grossberg, M., Kaupmees, L., Dedova, T., Timmo, K., Ernits, K., Kois, J., Acik, Oja, Danilson, M., Bereznev, S., 2008. Research in solar cell technologies at Tallinn University of Technology. Thin Solid Films 516, 7125–7134.

Mellikov, E., Meissner, D., Varema, T., Altosaar, M., Kauk, M., Volubujeva, O., Raudoja, J., Timmo, K., Danilson, M., 2009. Monograin materials for solar cells. Solar Energy Materials & Solar Cells 93, 65–68.

J.E. Phillips, W.N. Shafarman, E. Shan, Evidence for amorphous like behavior in small grain thin film polycrystalline solar cells, in: Proc. IEEE First WCPEC (24th IEEE PVSC), 1994, pp. 303–306.

Rau, U., Schock, H.W., 1999. Electronic properties of Cu(In, Ga)Se2 heterojunction solar cells–recent achievements, current understanding, and future challenges. Applied Physics A 69, 131–147.

Singh, P., Singh, S.N., Lal, M., Husain, M., 2008. Temperature dependence of I–V characteristics and performance parameters of silicon solar cell. Solar Energy Materials & Solar Cells 92, 1611–1616.

Skoplaki, E., Palyvos, J.A., 2009. On the temperature dependence of photovoltaic module electrical performance: a review of efficiency/power correlations. Solar Energy 83, 614–624.

Würfel, P., 2005. Physics of Solar Cells: From Principles to New Concepts. Wiley, VCH.